ELSEVIER

Chemical Geology 229 (2006) 113 – 124

CHEMICAL GEOLOGY
INCLUDING
ISOTOPE GEOSCIENCE

www.elsevier.com/locate/chemgeo

Water solubility and speciation in shoshonitic and latitic melt composition from Campi Flegrei Caldera (Italy)

V. Di Matteo [a,*], A. Mangiacapra [a,b], D.B. Dingwell [a], G. Orsi [b]

[a] *Department of Earth and Environmental Science, University of Munich, Theresienstr. 41/III 80333 München, Germany*
[b] *Instituto Nazionale di Geofisica e Vulcanologia-Osservatorio Vesuviano-via Diocleziano 328 Napoli, Italy*

Accepted 6 January 2006

Abstract

We report new data on water solubility in two melt compositions representative of volcanic units of the Campi Flegrei Caldera (Italy). The first composition is a primitive shoshonite and the second one is a more evolved latitic composition that have been chosen because of their less evolved nature compared to the other erupted products of Campi Flegrei. Water solubility was investigated at pressures from 25 to 200 MPa and 1200 °C following synthesis in an Internal Heated Pressure Vessel (IHPV). The glasses obtained from water-saturated experiments were analysed using both Fourier Transform Infra Red spectroscopy (FTIR) and Karl Fischer Titration (KFT). KFT was used as an independent method to obtain water concentration for the calibration of molar absorptivities of infrared bands at ~3550 cm^{-1} (total water), ~4500 cm^{-1} (hydroxyl groups) and ~5200 cm^{-1} (molecular water).

Water solubility in the shoshonitic melts is similar to that of a basalt while a slightly higher water solubility is observed for the latitic composition.

As regards the speciation, we have investigated the water speciation for the shoshonitic composition only and we have made a comparison between the data resulting using different molar absorptivities obtained for basaltic compositions similar to our shoshonite.

Keywords: Water solubility; Shoshonitic melts; Latitic melts; FTIR; Molar absorptivity; Water speciation

1. Introduction

Water is the most abundant volatile in magmas where it is commonly dissolved in up to several weight percent depending on the melt composition, pressure, temperature and degree of saturation. The presence of dissolved water in magmas affects phase equilibria and crystallization path (e.g. Yoder, 1969; Eggler, 1972; Kushiro, 1972; Yoder, 1973), redox equilibria of iron (e.g. Osborn, 1959; Moore et al., 1995; Gaillard et al., 2001), density (e.g. Lange and Carmichael, 1987; Richet et al., 2000), viscosity (e.g. Kushiro, 1978; Dingwell et al., 1996; Richet et al., 1996), diffusive mobility of melt chemical species (e.g. Watson, 1994) and electrical conductivity (e.g. Lebedev and Khitarov, 1964; Kushiro, 1978). In order to better understand the influence of water on both chemical and physical magma properties, the solubility of water in different silicate melts has been widely investigated (e.g. Goranson, 1931, 1936; Hamilton et al., 1964; Burnham and Davis, 1971, 1974; Burnham, 1974, 1975; Dingwell et al., 1984; Silver et

* Corresponding author.
E-mail address: matteo@min.uni-muenchen.de (V. Di Matteo).

0009-2541/$ - see front matter © 2006 Elsevier B.V. All rights reserved.
doi:10.1016/j.chemgeo.2006.01.015

al., 1990; Holtz et al., 1992; Blank et al., 1993; Dixon et al., 1995; Holtz et al., 1995; Carroll and Blank, 1997; Dingwell et al., 1997; Moore et al., 1998; Zhang, 1999; Zeng et al., 2000; Behrens and Jantos, 2001; Tamic et al., 2001). A natural consequence of such experimental efforts has been the production of models of water solubility in silicate melts based on the composition and the thermodynamic properties of the melts (Burnham, 1974, 1975; Papale, 1997; Moore et al., 1998).

Strictly connected to the effect of water on melt properties is the question of how the water is incorporated in the atomic structure of the melt. Water dissolves in silicate melts at least as two different species: molecular water (H_2O_{mol}) and hydroxyl groups (OH) (Scholze, 1960; Orlova, 1962; Ostroviskiy et al., 1964; Bartholomew et al., 1980; Stolper, 1982a,b; Newman et al., 1986; Nowak and Berhens, 1995; Zhang et al., 1995; Shen and Keppler, 1995; Nowak et al., 1996; Whiters et al., 1999; Nowak and Berhens, 2001; Behrens and Nowak, 2003). The relative abundance of molecular and hydroxyl dissolved water species can be described by the equilibrium reaction reported in Stolper (1982a):

$$H_2O_{mol}(melt) + O°(melt) = 2OH(melt) \quad (1)$$

where O° refers to a bridging oxygen and OH represent an OH group attached to a silicate polymer.

Using FTIR data from glasses, Stolper (1982a,b) presented evidence for the presence of molecular water as well as OH not only in the melt, but also in the glasses quenched from natural melts. Speculation on the temperature dependence of reaction (1) was replaced by a quantitative analysis by Dingwell and Webb (1990). The original fictive temperature analysis of the quench rate dependence of water speciation was quantitatively confirmed by successive in situ studies (Nowak and Berhens, 1995; Zhang et al., 1995; Shen and Keppler, 1995; Nowak et al., 1996). All of these studies demonstrated that the water speciation in the glass is not representative of the speciation in the melt at very high temperature but rather at the glass transition temperature. The stability of molecular water in the melt at high temperature has been demonstrated by in situ IR spectroscopy (Nowak and Berhens, 1995; Behrens and Nowak, 2003), but these studies all provide consistent evidence that the concentration of molecular water in the melt is much lower than in the glass and decreases systematically with increasing temperature.

Even if water solubility has been widely investigated in several melt compositions (especially rhyolitic and basaltic ones, but also some data exist for andesitic, basanitic, phonolitic or trachytic ones), there are no data on water solubility in shoshonitic and latitic melts, two compositions that we have chosen for this work because of their importance in the magmatic evolution of the products of the Campi Flegrei Caldera (Rosi and Sbrana, 1987). We have then investigated water solubility and speciation in natural shoshonitic and latitic melts and calibrated the molar absorptivity for the three water-related vibrating bands (~3500, ~4500 and ~5200 cm^{-1}). The solubility curve has been investigated at 1200 °C in the pressure range from 25 to 200 MPa. Water solubility in the latitic melts is higher than in the shoshonitic melt, as was anticipated due to its bulk composition.

2. Starting material and experimental methods

The two investigated compositions are a shoshonite from the unit 2a of the Minopoli 2 eruption and a latite from Fondo Riccio eruption of Campi Flegrei. Both eruptions occurred between 12 and 9.5 ka (Di Vito et al., 1999) and are peculiar of Campi Flegrei activity because their products present the less evolved compositions compared to those usually resulting from the different eruptions of the area. For a detailed geological, volcanological and chemical descriptions of these eruptions refer to Di Vito et al. (1999), D'Antonio et al. (1999) and Pappalardo et al. (2002). Compositions of the experimental starting materials are reported in Table 1.

Table 1
Chemical analyses of starting compositions and of the three different basalts recalled in the paper for comparison with our data

Oxide	Shoshonite Minopoli 2a[a]	Latite Fondoriccio[a]	MORB Basalt[b]	High Al-Basalt[c]	MORB Basalt[d]
SiO_2	51.8	53.8	50.8	51.84	49.64
TiO_2	0.84	0.87	–	1.39	0.87
Al_2O_3	15.39	17.67	13.7	17.08	16.07
FeO	7.21	6.9	12.4	10.2	8.63
MnO	0.16	0.15		0.18	0.15
MgO	5.7	2.43	6.67	5.32	9.77
CaO	10.9	5.83	11.5	10	14.44
Na_2O	2.04	4.34	2.68	2.87	2.28
K_2O	3.28	3.82	0.15	0.79	0.08
P_2O_5	0.47	0.58	0.19	0.33	–
LOI	0.6	1.53		–	–
Total	98.4	99.5		100	101.93
ε_{4500}				0.85	0.52
ε_{5200}				0.84	0.61

[a] The analyses of the samples have been performed at the Department of Earth and Environmental Science, University of Munich, (Germany) using a CAMECA SX50 and beam conditions of 10 nA and 15 keV. The analyses are consistent with the whole rock analyses reported in D'Antonio et al. (1999).
[b] Analyses from Dixon et al. (1995).
[c] Analyses from Yamashita et al. (1997).
[d] Analyses from Ohlhorst et al. (2001).

Starting material consists of whole rock, finely powdered by crushing and grinding in an agate mortar. Each experiment consisted of 100–150 mg of powder together with variable amount of distilled water (up to 7 wt.%) loaded into Pt capsules. The capsules were weighed after each addition of material and then sealed by welding. To verify that water was not lost during welding, a weight check after annealing to 110 °C was performed. The water content of individual capsules was varied as a function of the desired experimental pressure.

The experiments were run at the Department for Earth and Environmental Science in Munich (Germany) using an Internally Heated Pressure Vessel. Experimental temperatures were set to 1200 °C, to ensure the superliquidus condition for our compositions. Because of the use of Pt capsules, each experiment was run for 24 h that results to be the time necessary to obtain water homogeneity inside the samples and to limit iron-loss, as resulting by laboratory experience (Dixon et al., 1995). The oxidation condition of the apparatus was NNO+3, the typical hydrogen pressure at intrinsic condition of the IHPV when no additional input of hydrogen is added with the pressure medium. The applied pressure ranges from 25 to 200 MPa.

Experimental conditions for each sample are reported in Table 2.

Table 2
Experimental data

Sample	Temp (°C)	P (MPa)	D (h)	ρ (g/l)	A_{3550} (μm^{-1})	A_{4500} (μm^{-1})	A_{5200} (μm^{-1})	H_2O_{tot} [a]	H_2O_{tot} [b]	H_2O KFT	Notes
SHO 2	1200	52	24	2658	–	0.00017	0.00012	–	2.27 (0.01)	2.26 (0.03)	Glass
SHO 3	1200	52	24	2663	–	0.00101	0.00011	–	2.08 (0.06)	2.05 (0.06)	Glass
SHO 4	1200	52	24	2664	–	0.00015	0.0001	–	1.99 (0.05)	2 (0.06)	~1% opaques
SHO 5	1200	25	24	2682	0.0108	–	–	1.21 (0.06)	–	1.12 (0.04)	<2% opaques
SHO 6	1200	25	24	2685	0.0041	–	–	1.04 (0.04)	–	1.01 (0.06)	
SHO 7	1200	100	24	2642	–	0.00027	0.00020	–	3.13 (0.08)	3.24 (0.04)	<2% opaques
SHO 8	1200	60	24	2648	–	0.00018	0.0010	–	2.79 (0.07)	2.67 (0.03)	~1% opaques
SHO 9	1200	170	24	2621	–	0.0001	0.00041	–	3.86 (0.004)	4.13 (0.08)	<2% crystals
SHO 10	1200	170	24	2628	0.0330	–	–	3.78 (0.00)	–	3.86 (0.06)	Glass
SHO 12	1200	200	24	2614	–	0.00014	0.00042	–	4.32 (0.03)	4.4 (0.05)	Glass
LAT 1	1200	60	24	2575	0.0156	–	–	2.62 (0.09)	–	2.57 (0.05)	~1% opaques
LAT 2	1200	60	24	2665	0.217	–	–	2.45 (0.05)	–	2.52 (0.05)	~1% opaques
LAT 3	1200	60	24	2577	0.208	–	–	2.42 (0.06)	–	2.49 (0.05)	Glass
LAT 5	1200	52	24	2580	–	–	–	–		2.43 (0.05)	~1% opaques
LAT 6	1200	52	24	2578	0.204	–	–	2.37 (0.06)	–	2.43 (0.05)	Glass
LAT 7	1200	52	24	2578	0.207	–	–	2.42 (0.06)	–	2.37 (0.06)	Glass
LAT 9	1200	100	24	2558	0.0274	–	–	3.22 (0.01)	–	3.27 (0.06)	Glass
LAT 10	1200	100	24	2559	0.0291	–	–	3.41 (0.04)	–	3.45 (0.05)	Glass
LAT 11	1200	170	24	2535	0.0391	–	–	4.63 (0.06)	–	4.79 (0.05)	<2% crystals
LAT 12	1200	170	24	–	–	–	–	–	–	4.73 (0.05)	Glass
LAT 13	1200	200	24	2555	–	0.00017	0.00046	–	5.04 (0.04)		Glass
LAT 14	1200	200	24	2648	–	–	–	–	–	5.2 (0.04)	~1% opaques
LAT 15	1200	150	24	2648	–	0.00014	0.00042	–	4.23 (0.02)		Glass

SHO=shoshonite; LAT=latite; Temp=temperature (accuracy ±5 °C); P=pressure (accuracy ±2 MPa) ; D=duration of the experiment; ρ=calculated density (see text for details); A (μm^{-1})=absorbance at the different wave number/thickness of the samples. For both shoshonitic and latitic composition we have used the same ε_{3550}, ε_{4500} and ε_{5200} of 60, 0.81 and 0.93 l mol^{-1} cm^{-1}, respectively, as obtained from the calibration—see Section 3. Values in parenthesis represent the standard deviation of the calculated water.
Oxidation conditions of the IHPV=NNO+3.

[a] Refers to total water calculated using FTIR A_{3550} absorption peak.

[b] Refers to total water calculated using FTIR A_{4500} and A_{5200} absorption peaks.

After the quench (quench rate ~5°/s at the glass transition temperature), capsules were weighed to verify that they had remained sealed during the experiment and no weight loss had occurred. The run-product glasses have been examined under a binocular microscope: samples typically consisted of dark glasses, bubble free. In some cases, the synthetic products were characterized by the presence of small amounts of opaque oxides as reported in Table 2. Some glasses were crystallized, so they have been discarded for the investigation of water solubility and are not reported in the tables.

All the obtained glasses were divided into two parts: one part was used for the FTIR measurements and the other for the Karl Fischer Titration (KFT) analyses.

2.1. Karl Fischer Titration (KFT) and Fourier-Transform Infra Red (FTIR)

KFT analysis have been performed at the Institute of Mineralogy of the University of Hannover (Germany). KFT method is used to determine total water content in samples typically weighing 15–20 mg. The water is extracted by heating the samples from room temperature to about 1300 °C. The duration of the extraction lasts from 7 to 15 min depending on the heating programme that consists of different heating steps each lasting few minutes (Behrens, 1995; Ohlhorst et al., 2001). Subsequent FTIR measurements of the glasses confirm that the water in the measured samples has been systematically extracted by KFT. The residual water content depends on the investigated composition and on the initial water content. Usually, between 0.10 and 0.15 wt.% of unextracted H_2O is found in samples containing initially more than 1.5 wt.% H_2O (Behrens, 1995; Ohlhorst et al., 2001; Behrens and Stuke, 2003). For each of our samples, the unextracted water was measured by re-melting the samples after KFT using IHPV and measuring the residual water by FTIR.

A complete description of the KFT method is given by Behrens (1995). KFT results for our samples are given in Table 2.

FTIR analyses have been performed at the Department for Earth and Environmental Science in Munich (Germany). A Bruker Equinox 55 FTIR spectrometer has been used with CaF_2 beamsplitter, MCT/A detector and white-light source to obtain the spectra at 4 cm^{-1} resolution using 128 scans. For the analysis, the samples were placed on a KBr crystal plate that is transparent to the infrared beam and analysed in several points (from 3 to 15 points per sample, also using different chips of the same sample to better investigate the homogeneity of the sample) using a spot size of 100 μm. The points were chosen using a Bruker Irscope II microscope connected to the spectrometer. Thickness was measured using a Mitutoyo digital displacement gauge (accuracy ±2 μm).

Water contents were determined from the peak height of the band at ~3550 cm^{-1} (proportional to total water) and the combination bands at ~4500 cm^{-1} (proportional to hydroxyl group abundance) and ~5200 cm^{-1} (proportional to molecular water abundance) (Stolper, 1982a,b; Newman et al., 1986). The two separate contributions of molecular water and hydroxyl groups make it possible to obtain information on the speciation of water in the analysed glass. For all these bands, we have calibrated the linear molar absorptivity as reported below.

3. FTIR calibration, water solubility and speciation

Using the results of KFT, we have calibrated the molar absorptivity ε_{3550} for our shoshonitic and latitic samples using the Beer–Lambert Law:

$$c = \frac{18.02A}{t\rho\varepsilon} * 100 \quad (2)$$

where c is the water concentration in wt.%; 18.02 is the molecular weight of water; A is the height of the absorbance

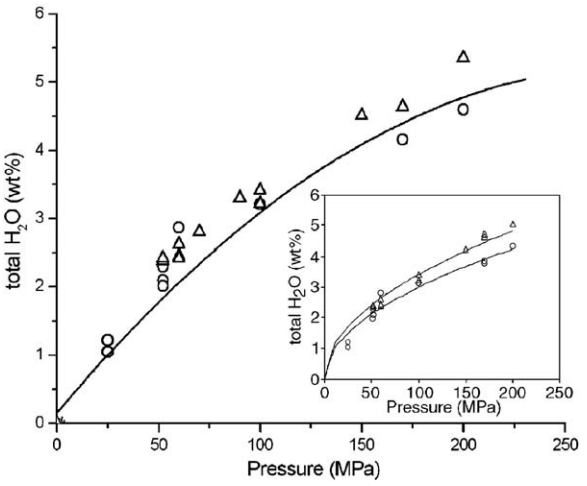

Fig. 1. Water solubility of shoshonitic and latitic composition at different pressures. Open circles: shoshonitic composition; open triangles: latitic composition; solid line: basaltic composition from Dixon et al. (1995). Data for shoshonite and latite are from FTIR: they have been calculated considering the 3550 cm^{-1} vibration peak for total water and molar absorptivity of 60 l mol^{-1} cm^{-1}. The inset shows the two fit curves for shoshonitic and latitic compositions. The equations of the two curves are H_2O (wt.%) = $0.341P^{0.5}$ (R^2 = 0.99; mean error = 0.197) for the shoshonitic composition and H_2O (wt.%) = $0.3P^{0.5}$ (R^2 = 0.95; mean error = 0.136) for the latitic composition.

peak; t is the sample thickness (cm), ρ is the density (g/l) and ε is the molar absorptivity (l mol^{-1} cm^{-1}).

The density of the glasses (ρ) has been calculated using the method described in Lange and Carmichael (1987) using a partial molar volume for water of 12 cm^3/mol (Richet et al., 2000). The calculated density for each sample is reported in Table 2. The results of the anhydrous and hydrated glass density have been compared with the measured densities of the basaltic composition used by Ohlhorst et al. (2001) and Yamashita et al. (1997). These authors found values that range from 2688 g/l to 2790 g/l depending on the compositions and on water content. Our calculated densities are lower being 2707 g/l for the anhydrous composition and from 2610 to 2685 g/l decreasing water content, but it must be stressed that our samples are more alkali-rich. The reliability of the calculated hydrate density has been verified comparing our variation of density for different water content with those from the references: measured and calculated densities are within 1% and such small variations have a negligible effect on calculated water content.

Heights of the absorbance peaks at 3550 cm^{-1} were measured considering the flexicurve or French curve baseline correction (Ohlhorst et al., 2001). The equivalence of different baseline corrections for the determination of total water content has been shown by several studies (e.g. Whiters et al., 1999; Ohlhorst et al., 2001). However, it must be emphasized that the results on the species concentration are sensitive to the choice of the baseline (Ohlhorst et al., 2001).

The molar absorptivity ε_{3550} obtained from Eq. (1) results of 60±2 l mol^{-1} cm^{-1} both for the shoshonitic and the latitic melt composition. This value is the same (60±10%) obtained by Stolper (1982b) in his FTIR calibration for compositions that range from rhyolitic to basaltic glasses.

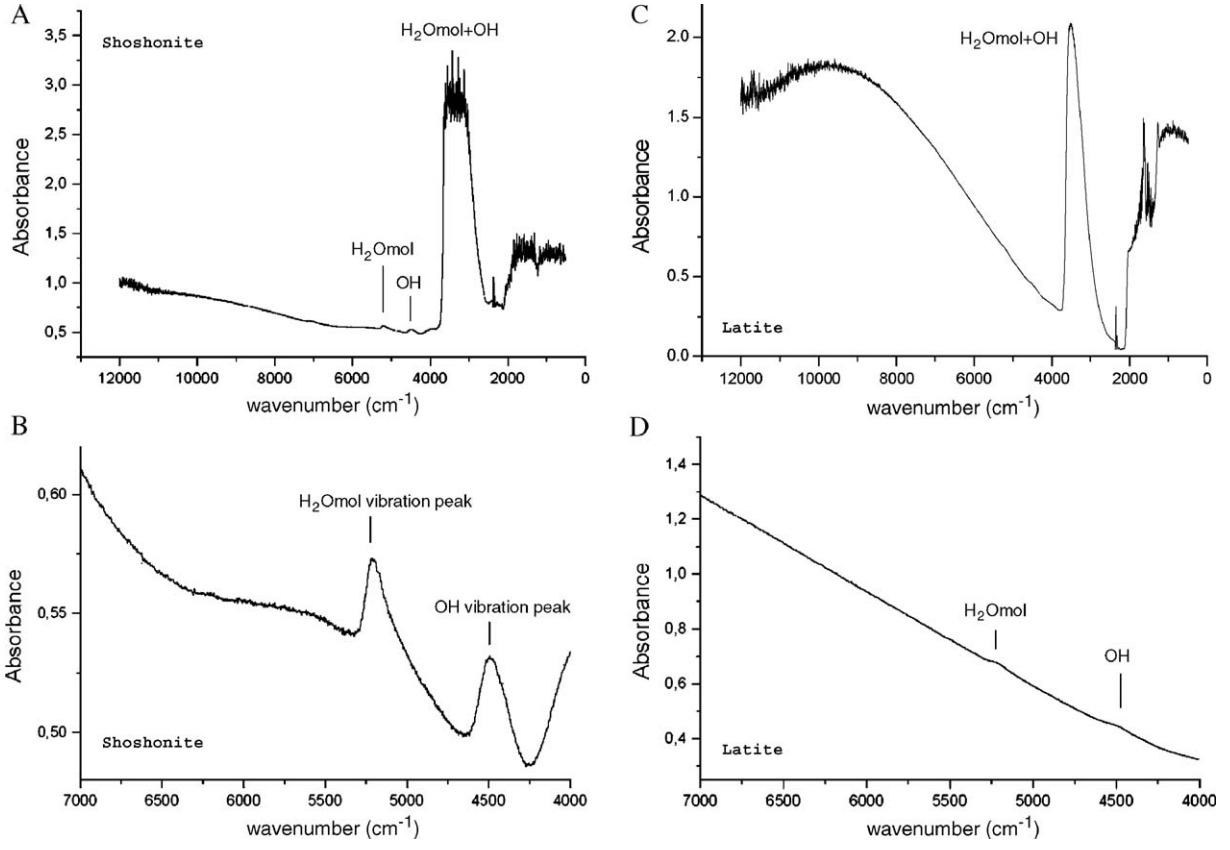

Fig. 2. Spectra for the investigated compositions. (A) Total NIR absorption spectrum for the shoshonite. The saturation of the 3550 cm^{-1} adsorption peak for total water in this case does not allow to use this peak for the calculation of the absorbance. (B) Zoom of the spectrum for the shoshonite in the wave number range of 7000–4000 cm^{-1} that is the range of vibration of hydroxyl groups and molecular water. (C) Total NIR absorption spectrum for the latite. Again the 3550 cm^{-1} adsorption peak is not useful for the calculation of the water content in the investigated sample. (D) Zoom of the spectrum for the latite in the wave number range of 7000–4000 cm^{-1}, range of vibration of hydroxyl groups and molecular water. In this case it is not possible to investigate the separate contributions of H_2O_{mol} and OH groups as the vibration peaks are not visible.

Table 3
Values used for calculation of water speciation in the investigated glasses

Sample	T (°C)	ρ (g/l)	A_{4500}	A_{5200}	OH[a] (wt.%)	H_2O_{mol}[a] (wt.%)	H_2O_{tot}[a] (wt.%)	OH[b] (wt.%)	H_2O_{mol}[b] (wt.%)	H_2O_{tot}[b] (wt.%)	OH[c] (wt.%)	H_2O_{mol}[c] (wt.%)	H_2O_{tot}[c] (wt.%)
SHO2(1)	55	2707	0.0096	0.0065	1.37	0.94	2.30	2.23	1.29	3.52	1.43	0.85	2.28
SHO2(2)	55	2707	0.0094	0.0067	1.34	0.97	2.30	2.19	1.33	3.52	1.40	0.87	2.28
SHO2(3)	50	2707	0.0087	0.0058	1.36	0.92	2.28	2.23	1.27	3.49	1.43	0.83	2.26
SHO 3(1)	89	2707	0.0136	0.0098	1.20	0.87	2.07	1.96	1.20	3.16	1.26	0.78	2.05
SHO 3(2)	100	2707	0.0165	0.0106	1.29	0.84	2.13	2.11	1.16	3.27	1.35	0.76	2.11
SHO 3(4)	110	2707	0.0184	0.0115	1.31	0.83	2.14	2.14	1.14	3.28	1.38	0.75	2.13
SHO 3(5)	119	2707	0.0198	0.013	1.30	0.87	2.17	2.13	1.19	3.32	1.37	0.78	2.15
SHO 3(6)	90	2707	0.014	0.01	1.22	0.88	2.10	1.99	1.21	3.20	1.28	0.79	2.07
SHO 3(7)	121	2707	0.0204	0.011	1.32	0.72	2.04	2.16	0.99	3.15	1.39	0.65	2.04
SHO 3(8)	113	2707	0.0187	0.011	1.30	0.77	2.07	2.12	1.06	3.18	1.36	0.70	2.05
SHO 3(9)	103	2707	0.015	0.0107	1.14	0.82	1.96	1.86	1.13	3.00	1.19	0.74	1.93
SHO 3(10)	78	2707	0.0116	0.0097	1.16	0.99	2.15	1.90	1.36	3.26	1.22	0.89	2.11
SHO 3(11)	90	2707	0.0152	0.0096	1.32	0.85	2.17	2.16	1.16	3.33	1.40	0.76	2.16
SHO 4(1)	77	2707	0.013	0.007	1.32	0.72	2.04	2.16	0.99	3.15	1.39	0.65	2.04
SHO 4(2)	85	2707	0.011	0.0102	1.01	0.95	1.96	1.66	1.31	2.97	1.06	0.85	1.91
SHO 4(3)	84	2707	0.013	0.008	1.21	0.75	1.97	1.98	1.04	3.02	1.28	0.68	1.96
SHO 4(4)	75	2707	0.011	0.0084	1.15	0.89	2.04	1.88	1.22	3.10	1.21	0.80	2.01
SHO 4(5)	70	2707	0.011	0.007	1.23	0.79	2.02	2.01	1.09	3.10	1.29	0.72	2.01
SHO 7(1)	270	2707	0.0499	0.0558	1.45	1.64	3.09	2.37	2.26	4.62	1.52	1.48	3.01
SHO 7(2)	266	2707	0.053	0.0545	1.56	1.62	3.18	2.55	2.24	4.79	1.64	1.46	3.10
SHO 7(3)	268	2707	0.0545	0.0542	1.59	1.60	3.20	2.60	2.21	4.81	1.68	1.45	3.13
SHO 7(4)	275	2707	0.0594	0.0521	1.69	1.50	3.19	2.77	2.07	4.83	1.77	1.36	3.13
SHO 7(5)	277	2707	0.0591	0.0524	1.67	1.50	3.17	2.73	2.06	4.80	1.75	1.35	3.11
SHO 7(6)	273	2707	0.052	0.0552	1.49	1.60	3.09	2.44	2.21	4.64	1.56	1.45	3.01
SHO 7(7)	274	2707	0.0548	0.0558	1.57	1.61	3.18	2.56	2.22	4.78	1.64	1.46	3.10
SHO 7(8)	308	2707	0.0609	0.0683	1.55	1.76	3.31	2.53	2.42	4.95	1.63	1.59	3.21
SHO 7(9)	308	2707	0.0617	0.0688	1.57	1.77	3.34	2.56	2.44	5.00	1.65	1.60	3.25
SHO 7(10)	278	2707	0.059	0.0528	1.66	1.51	3.17	2.72	2.07	4.79	1.74	1.36	3.10
SHO 7(11)	290	2707	0.0586	0.0602	1.58	1.65	3.23	2.59	2.27	4.85	1.66	1.49	3.15
SHO 7(12)	303	2707	0.0598	0.0678	1.55	1.77	3.32	2.53	2.44	4.97	1.62	1.60	3.22
SHO 7(13)	273	2707	0.0541	0.0545	1.55	1.58	3.13	2.54	2.18	4.72	1.63	1.43	3.06
SHO 7(14)	297	2707	0.0599	0.0636	1.58	1.70	3.28	2.58	2.34	4.92	1.66	1.54	3.20
SHO 8(1)	193	2707	0.0342	0.0339	1.39	1.39	2.78	2.27	1.92	4.19	1.46	1.26	2.72
SHO 8(2)	208	2707	0.037	0.041	1.39	1.56	2.96	2.28	2.15	4.43	1.46	1.41	2.87
SHO 8(3)	194	2707	0.0353	0.0344	1.43	1.41	2.83	2.33	1.94	4.26	1.50	1.27	2.77
SHO 8(4)	218	2707	0.0408	0.042	1.47	1.53	2.99	2.40	2.10	4.50	1.54	1.38	2.92
SHO 8(5)	247	2707	0.0438	0.043	1.39	1.38	2.77	2.27	1.90	4.17	1.46	1.25	2.71
SHO 8(6)	259	2707	0.0456	0.047	1.38	1.44	2.82	2.25	1.98	4.23	1.45	1.30	2.74
SHO 8(7)	253	2707	0.0444	0.0448	1.37	1.40	2.78	2.25	1.93	4.18	1.45	1.27	2.72
SHO 8(8)	265	2707	0.05	0.05	1.48	1.50	2.97	2.42	2.06	4.47	1.55	1.35	2.90
SHO 8(9)	262	2707	0.0474	0.0464	1.42	1.40	2.82	2.32	1.93	4.25	1.49	1.27	2.75
SHO 8(10)	300	2707	0.055	0.056	1.44	1.48	2.92	2.35	2.04	4.38	1.51	1.34	2.84
SHO 8(11)	300	2707	0.0528	0.0567	1.38	1.50	2.88	2.25	2.06	4.32	1.45	1.36	2.81
SHO 8(12)	300	2707	0.0536	0.052	1.40	1.37	2.77	2.29	1.89	4.18	1.47	1.24	2.71
SHO 8(13)	300	2707	0.0558	0.055	1.46	1.45	2.91	2.38	2.00	4.38	1.53	1.31	2.84
SHO 8(14)	300	2707	0.0542	0.0542	1.41	1.43	2.85	2.31	1.97	4.28	1.49	1.30	2.79
SHO 8(15)	300	2707	0.0549	0.054	1.43	1.43	2.86	2.34	1.96	4.31	1.50	1.29	2.79
SHO 9(1)	34	2617	0.0045	0.01295	1.07	3.12	4.19	1.75	4.30	6.05	0.87	3.00	3.87
SHO 9(2)	34	2617	0.0042	0.0131	1.00	3.16	4.16	1.64	4.35	5.98	0.67	3.17	3.85
SHO 9(3)	35	2617	0.0043	0.0133	1.00	3.11	4.11	1.63	4.29	5.92	1.04	2.83	3.87
SHO 9(4)	31	2617	0.0038	0.012	0.99	3.17	4.17	1.62	4.37	5.99	0.77	3.10	3.87
SHO 12(1)	92	2707	0.014	0.0388	1.19	3.34	4.53	1.95	4.60	6.55	1.25	3.03	4.28
SHO 12(2)	99	2707	0.0142	0.0436	1.12	3.49	4.61	1.84	4.81	6.64	1.19	3.17	4.35
SHO 12(3)	88	2707	0.0111	0.0406	0.99	3.66	4.64	1.61	5.03	6.65	1.04	3.31	4.35
SHO 12(4)	88	2707	0.011	0.0404	0.98	3.64	4.62	1.60	5.01	6.61	1.03	3.29	4.32
SHO 12(5)	97	2707	0.014	0.0431	1.13	3.52	4.65	1.85	4.85	6.70	1.18	3.17	4.35

Table 3 (*continued*)

Sample	T (°C)	ρ (g/l)	A_{4500}	A_{5200}	OH[a] (wt.%)	H_2O_{mol}[a] (wt.%)	H_2O_{tot}[a] (wt.%)	OH[b] (wt.%)	H_2O_{mol}[b] (wt.%)	H_2O_{tot}[b] (wt.%)	OH[c] (wt.%)	H_2O_{mol}[c] (wt.%)	H_2O_{tot}[c] (wt.%)
SHO 12(6)	92	2707	0.0139	0.0387	1.18	3.33	4.52	1.93	4.59	6.52	1.25	3.02	4.26
LAT13(1)	30	2555	0.005	0.014	1.38	3.92	5.30	2.26	5.40	7.66	1.45	3.54	4.99
LAT13(2)	30	2555	0.0053	0.014	1.47	3.92	5.38	2.40	5.40	7.79	1.54	3.54	5.08
LAT13(3)	30	2555	0.0052	0.014	1.44	3.92	5.36	2.35	5.40	7.75	1.51	3.54	5.05
LAT 15(1)	40	2648	0.007	0.015	1.40	3.04	4.44	2.29	4.18	6.47	1.47	2.74	4.21
LAT 15(2)	30	2648	0.003	0.014	0.80	3.78	4.58	1.31	5.21	6.51	0.84	3.41	4.25
LAT 15(3)	30	2648	0.003	0.014	0.80	3.78	4.58	1.31	5.21	6.51	0.84	3.41	4.25
LAT 15(4)	40	2648	0.007	0.015	1.40	3.04	4.44	2.29	4.18	6.47	1.47	2.74	4.21

Numbers in parenthesis refers to the measured spot of the same sample. SHO = shoshonite; LAT = Latite; T = temperature; ρ = density.

[a] Data resulting using the molar absorptivities from Yamashita et al. (1997).

[b] Data resulting using the molar absorptivities from Ohlhorst et al. (2001).

[c] Data resulting using the molar absorptivities from this calibration.

Once the molar absorptivities ε_{3500} for the two investigated composition have been obtained, it is possible to calculate the water content for each sample.

Fig. 1 reports the two solubility curves in the investigate pressure range of 25–200 MPa. The solubility curve of a basalt from Dixon et al. (1995) (composition in Table 1) is also reported for comparison. The slightly higher water solubility in the latitic composition with respect to the shoshonitic one at our experimental conditions can be explained considering its higher silica and sodium content. In fact, it is known (Goranson, 1931, 1936; Hamilton et al., 1964) that higher silica content magmas are able to dissolve more water inside their structure. Also the influence of sodium on water solubility has been investigated by several authors (e.g. Holtz et al., 1995; Dingwell et al., 1997) who found evidence that water solubility is higher for those melts that have similar composition but higher wt.% of sodium. But the relationship between the anhydrous composition and water solubility is too complex to be explained with only two compositionally different sets of data, so here we only report the fit curve equation for the two compositions, that are: H_2O (wt.%) = $0.341P^{0.5}$ (R^2 = 0.99; mean error = 0.197) for the shoshonitic composition and H_2O (wt.%) = $0.3P^{0.5}$ (R^2 = 0.95; mean error = 0.136) for the latitic composition, where the pressure is expressed in MPa (Fig. 1, inset).

As regards water speciation, several studies (Keppler and Bagdassarov, 1993; Shen and Keppler, 1995; Nowak and Berhens, 1995; Whiters et al., 1999; Behrens and Nowak, 2003) confirm the proposal of Dingwell and Webb (1990) that the speciation of water in the glass is the result of the thermal history of the glass and that hydroxyl groups are the predominant species in the high temperature melt.

Thus, we recall that the speciation that is investigated in a quenched glass is not representative of the speciation in the high temperature melt, but rather the result of the thermal history of the glass.

Nevertheless, the investigation of the OH and H_2O combination bands is sometimes more suitable for water determination in water-rich samples (>2%wt H_2O). In fact for these samples, the fundamental OH stretching band vibrating at 3550 cm^{-1} becomes too intense and often saturated unless extremely thin sections (<30 μm) would be used for IR measurements.

Two typical spectra for the two different compositions studied are shown in Fig. 2A–D. Both shoshonitic and latitic glasses are characterized by spectra with a broad band from about 5600 cm^{-1} to higher wave number that are iron related bands (Rossman, 1988; Dixon et al., 1995; Ohlhorst et al., 2001). Because of the presence of iron oxides resulting from the quench, for most of the latitic glasses (except samples LAT5, LAT12 and LAT13), this band at 5600 cm^{-1} is superimposed by another very intense iron-related peak present at about 10 000 cm^{-1} (Rossman, 1988; Dixon et al., 1995) that does not allow recognition of the water vibration band at 5200 cm^{-1} and sometimes that at 4500 cm^{-1}. As a result, it was not possible to investigate water speciation in the latite glasses and the water in the glass was calculated using only the total water vibration peak at 3500 cm^{-1}.

The two vibration peaks of hydroxyl groups and molecular water occur in the range 4483–4505 cm^{-1} and 5205–5220 cm^{-1} for the shoshonitic glasses while they occur in the range 4426–4430 cm^{-1} and 5217–5230 cm^{-1} for the three latitic samples for which it was possible to recognize these peaks. The different values for vibrational peaks are not connected to different water content but appear to be related to the influence of the tail of the nearby peaks.

One of the greatest disadvantages in the use of FTIR for water content calculation is the necessity of the calibration for the molar absorptivities for each composition. In the case of our latitic samples, it is not possible to recognize the peak for the calibration of water speciation and we have calibrated molar absorptivities of the 4500 cm^{-1} and 5200 cm^{-1} only for the shoshonitic composition. The heights of the absorbing peak at 4500 and 5200 cm^{-1} are difficult to obtain because of the influence of the adjacent bands. The choice of a correct baseline in this case is fundamental. Ohlhorst et al. (2001) report the different results that can be obtained using different baselines. For our peak, we have used two Gaussian curves fitted to the iron-related band at about 5600 cm^{-1} and to the water-related band at about 4000 cm^{-1} (see Ohlhorst et al., 2001 for the description of the different baseline corrections methods). The absorbance values are reported in Table 2.

Molar absorptivity strongly depends on the anhydrous composition of the glass (McMillan, 1994; Dixon et al., 1995), therefore, prior to attempting any calibration, we tried to use some absorptivity values from the literature to see if they could also be used for our shoshonitic composition. For this, we used the molar absorptivities calculated by Ohlhorst et al. (2001) for an averaged primitive MORB and by Yamashita et al. (1997) for a high Al-basalt of arc magma composition. Both basalts have some oxide content close to our shoshonitic composition and differ for some others (Table 1). Notably however, the potassium content is very different from both of the reference compositions, as the shoshonite has a potassium content up to 4 wt.%. If the molar absorptivity is dependent on the anhydrous composition, then it should be possible to use one of these molar absorptivities to describe water speciation and total water content in our shoshonitic glasses.

The molar absorptivities of the two different basalts from Ohlhorst et al. (2001) and Yamashita et al. (1997) are reported in the Table 1 together with the chemical analyses of these compositions. In Table 3, the values of total water are reported and those of the two contributions of hydroxyl groups and molecular water obtained using the different values of molar absorptivity, while in Fig. 3 we report the speciation curves. It is possible to note that using the values of molar absorptivity

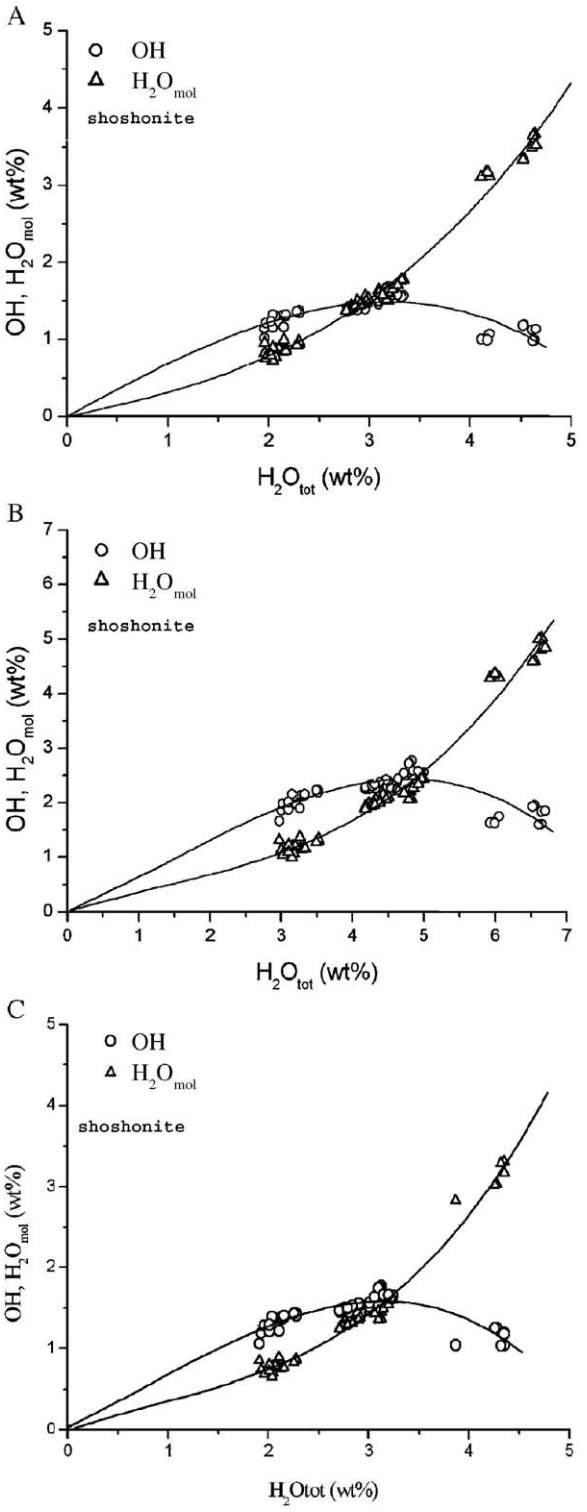

Fig. 3. (A) Water speciation for the shoshonitic composition calculated using the molar absorptivities of 0.85 l mol^{-1} cm^{-1} (ε_{4500}) and 0.84 l mol^{-1} cm^{-1} (ε_{5200}) from Yamashita et al. (1997). (B) Water speciation for shoshonitic composition calculated using the molar absorptivities of 0.52 l mol^{-1} cm^{-1} (ε_{4500}) and 0.61 l mol^{-1} cm^{-1} (ε_{5200}) from Ohlhorst et al. (2001). (C) Water speciation for shoshonitic composition calculated using the molar absorptivities of 0.61 l mol^{-1} cm^{-1} (ε_{4500}) and 0.99 l mol^{-1} cm^{-1} (ε_{5200}). Note that total water for (A) and (C) is similar, while the speciation result is slightly different.

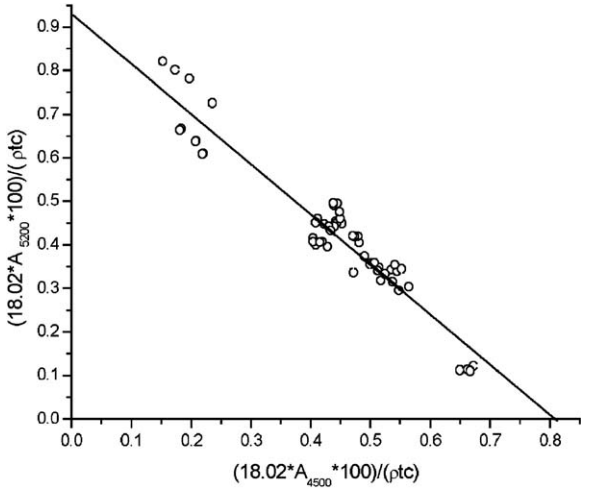

Fig. 4. Calibration plot used to determine the molar absorptivity for the NIR combination bands at 5200 cm^{-1} (molecular water) and 4500 cm^{-1} (hydroxyl groups). Molar absorptivities are given by the intercepts of the regression line with the Cartesian axes.

proposed by Ohlhorst et al. (2001), we have higher total water content if compared with those obtained using the molar absorptivities proposed by Yamashita et al. (1997). The molar absorptivity proposed by Yamashita et al. (1997) also gives water content closer to that obtained with KFT.

One explanation of the good correlation using the data from Yamashita et al. (1997) is that among the oxides that are similar to the shoshonitic compositions are CaO and MgO that are supposed to have an important role in the bond with the OH groups (Kohn et al., 1992; Schmidt et al., 2000, 2001). Therefore, if SiO_2 and Al_2O_3 can be considered similar in both the compositions from Ohlhorst et al. (2001) and Yamashita et al. (1997), the difference in these two oxides content can justify the validity of the molar absorptivity. The other element that can play an important role in the bond with OH group is the iron. The iron in the basalt from Yamashita et al. (1997) is clearly higher than those of the shoshonite and of the basalt from Ohlhorst et al. (2001), but this does not seem to have a significant influence on the molar absorptivity values possibly because the Fe^{2+}/Fe^{3+} in the structure is more important than the total iron.

The use of the two values of molar absorptivities of 0.85 for ε_{4500} and 0.84 for ε_{5200} (Yamashita et al., 1997) yields consistent information on total water content, but could be ambiguous for the speciation. To have more precise information on the speciation for our composition, a new calibration is required.

Again, for the calibration we need to apply the Beer–Lambert Law for both the OH and H_2O species:

$$c_{H_2O} = \frac{18.02 * A_{5200} * 100}{t\rho\varepsilon_{5200}} \quad (3)$$

$$c_{OH} = \frac{18.02 * A_{4500} * 100}{t\rho\varepsilon_{4500}} \quad (4)$$

where c_{H_2O} and c_{OH} are the concentration of molecular water and of hydroxyl groups (wt.%), A_{5200} and A_{4500} are the absorbances, t is the thickness (cm), ρ is the density (g/l) and ε_{5200} and ε_{4500} are the molar absorptivity coefficients (l mol^{-1} cm^{-1}). As the total water can be considered as the sum of molecular and hydroxyl species ($c_{water} = c_{H_2O} + c_{OH}$), we can rearrange Eqs. (3) and (4) to obtain:

$$\left(\frac{18.02 * A_{5200} * 100}{t\rho c_{H_2O}}\right) = \varepsilon_{H_2O} - \frac{\varepsilon_{H_2O}}{\varepsilon_{OH}}\left(\frac{18.02 * A_{OH} * 100}{t\rho c_{OH}}\right). \quad (5)$$

From this equation, it is possible to determine the values of the two molar absorptivities by plotting the values in parenthesis (normalized absorbances) against each other. The aligned positions of the values along a straight line shows that molar absorptivities are constant values and do not depend on the water content of the

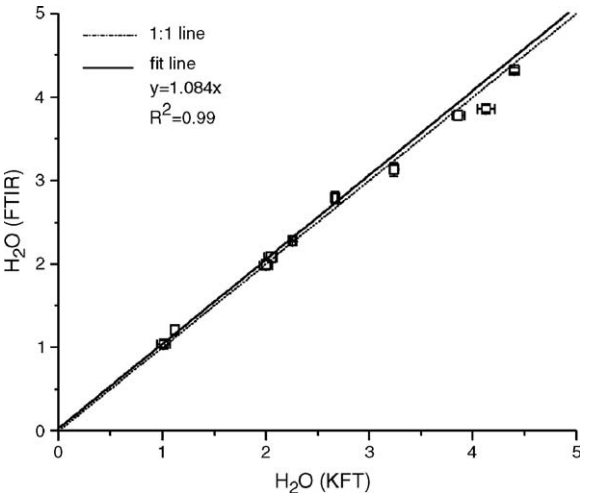

Fig. 5. Relationship between total water content (wt.%) measured with KFT and that calculated with FTIR using the molar absorptivities of $0.61_{-0.16}^{+0.20}$ l mol^{-1} cm^{-1} for ε_{4500} and 0.99–sub $_{0.17}^{+0.22}$ l mol^{-1} cm^{-1} for ε_{5200}. Both the 1:1 line and the equation of the fit line $y = 1.084x$ ($R^2 = 0.99$) are reported.

samples. The intercepts of the line obtained with the two axes gives the looked values that, in this case, result of $0.61^{+0.20}_{-0.16}$ l mol^{-1} cm^{-1} for ε_{4500} and $0.99^{+0.22}_{-0.17}$ l mol^{-1} cm^{-1} for ε_{5200} (Fig. 4). The consistence of these values is supported by the good agreement we found comparing total water content calculated using FTIR data with water content measured with KFT (Fig. 5).

It must be noted that while the water content is very similar to total water obtained using the molar absorptivities from Yamashita et al. (1997) the speciation is different and in particular the hydroxyl concentration is higher and the molecular water content is lower (Fig. 3C).

4. Conclusions

The FTIR calibration of the molar absorptivity for the shoshonitic and latitic composition has allowed the quantification of water concentrations in melts synthesized at 1200 °C and various pressures starting from natural products of Campi Flegrei volcanic activity.

The value found for the molar absorptivity for total water vibrating at about 3600 cm^{-1} is comparable to the 60 l mol^{-1} cm^{-1} ± 10% found by Stolper (1982a,b) for other silicate melts. As far as the molar absorptivities for the hydroxyl group and molecular water are concerned, we remark the difficulty in predicting these two values starting from the anhydrous composition. In fact, compositions having comparable content of some of the major oxides, can have different values of molar absorptivities and may fortuitously give comparable results of total water content, but do not yield any precise information on water speciation recorded at the glass transition temperature. This difference reflects the lack of reliable models for predicting how molar absorptivity varies with glass composition.

Using both the FTIR and the KFT, we have calculated the solubility of water for both shoshonitic and latitic compositions of interest for the volcanism of Campi Flegrei. For the shoshonitic melt, we found that the water solubility vs. pressure curve is close to that of a basalt while that of the latitic melt is slightly higher. The combination of data on water solubility and water amounts recorded in glassy inclusions hosted in minerals picked up from Minopoli 2 and Fondo Riccio volcanic units can give important information on the water in the magmatic chamber and on the depth and condition of formation of these two kinds of magma so peculiar in Campi Flegrei system. Working on olivine-hosted melt inclusions from the Minopoli 2 shoshonitic composition, Cecchetti et al. (2001) found up to 3 wt.% H_2O. According to such data, we can fix an upper limit to the origin depth of Minopoli 2 shoshonitic composition that can result to 100 MPa (~3.3 km of depth). Unfortunately, our data are not enough to fix also a lower depth limit of these shoshonitic compositions. In fact, for this purpose, more information on melt and glass inclusion is needed, possibly on both high pressure and lower pressure minerals that until now have never been investigated. Also the presence of other volatile species, in particular of magmatic CO_2 would be necessary to better constrain the depth of origin and the evolution of such a magma. All these additional information is obviously necessary for the understanding of chemical and physical processes occurring in the magma chamber and in particular for the definition of the thermo-barometric conditions at which they happen. Moreover, both the definitions of the depth of the magma chamber and of the water content are extremely important for the evaluation of the volcanic risk of the Campi Flegrei area.

For this, further detailed investigations of chemical and physical parameters such as oxidation state, viscosity and diffusion of chemical components in all magma compositions of Campi Flegrei are necessary to better constrain magma dynamics both inside the magma chamber and also during the conduit ascent.

Acknowledgement

The authors want to thank Roberto Isaia for the help during the sampling, Thomas Kunzmann, Renata Rafinska and Conrad Gennaro for the help in the use of the IHPV, Dennis Lemke for KFT measurements, Mike Carroll for suggestion in setting the experimental conditions, and an anonymous reviewer for the comments. A special thank to Harald Behrens for comments and for the improvement of the manuscript, Mac Rutherford for helpful review and to Jon Castro and Monica Piochi for final comments. This work was supported by Volcano Dynamics EU Research Training Network (HPRN-CT-2000-00060). **[RR] [RM]**

References

Bartholomew, R.F., Butler, B.L., Hoover, H.L., Wu, C.K., 1980. Infrared spectra of a water containing glass. J. Am. Ceram. Soc. 63, 481–485.

Behrens, H., 1995. Determination of water solubities in high-viscosity melts: an experimental study on $NaAlSi_3O_8$. Eur. J. Mineral. 7, 905–920.

Behrens, H., Jantos, N., 2001. The effect of anhydrous composition on water solubility in granitic melts. Am. Mineral. 86, 14–20.

Behrens, H., Nowak, M., 2003. Quantification of H_2O speciation in silicate glasses and melts by IR spectroscopy—in situ versus quench techniques. Phase Transit. 76 (1–2), 45–61.

Behrens, H., Stuke, A., 2003. Quantification of H_2O contents in silicate glasses using IR spectroscopy—a calibration based on

hydrous glasses analyzed by Karl–Fischer titration. Glass Sci. Technol. 76, 176–189.
Blank, J.G., Stolper, E.M., Carroll, M.R., 1993. Solubilities of carbon dioxide and water in rhyolitic melt at 850 °C and 750 bars. Earth Planet. Sci. Lett. 119, 27–36.
Burnham, C.W., 1974. $NaAlSi_3O_8$–H_2O solutions: a thermodynamic model for hydrous magmas. Bull. Soc. Fr. Mineral. Cristallogr. 97, 223–230.
Burnham, C.W., 1975. Water and magmas: a mixing model. Geochim. Cosmochim. Acta 39, 1077–1084.
Burnham, C.W., Davis, N.F., 1971. The role of H_2O in silicate melts: I. PVT reltions in the system $NaAlSi_3O_8$–H_2O to 10 kilobars and 1000 °C. Am. J. Sci. 270, 54–79.
Burnham, C.W., Davis, N.F., 1974. The role of H_2O in silicate melts: II. Thermodynamic and phase relations in the system $NaAlSi_3O_8$–H_2O to 10 kbars 700 °C–1100 °C. Am. J. Sci. 274, 902–940.
Carroll, M.R., Blank, J.G., 1997. The solubility of H_2O in phonolitic melts. Am. Mineral. 82, 1111–1115.
Cecchetti, A., Marianelli, P., Sbrana, A., 2001. A deep magma chamber beneath Campi Flegrei? Insights from melt inclusions. GNV-Framework Program 2000–2002: 1 year results. Oss. Vesuv. 59–65.
D'Antonio, M., Civetta, L., Orsi, G., Pappalardo, L., Piochi, M., Carandente, A., et al., 1999. The present state of the magmatic system of the Campi Flegrei caldera based on a reconstruction of its behavior in the past 12 ka. J. Volcanol. Geotherm. Res. 91, 247–268.
Dingwell, D.B., Webb, S.L., 1990. Relaxation in silicate melts. Eur. J. Mineral. 2, 427–449.
Dingwell, D.B., Harris, D.M., Scarfe, C.M., 1984. The solubility of H_2O in melts in the system SiO_2–Al_2O_3–Na_2O–K_2O at 1 to 2 kbars. J. Geol. 92, 387–395.
Dingwell, D.B., Romano, C., Hess, K.U., 1996. The effect of water on viscosity of a haplogranitic melt at P–T–X conditions relevant to silicic volcanism. Contrib. Mineral. Petrol. 124, 19–28.
Dingwell, D.B., Holtz, F., Bherens, H., 1997. The solubility of H_2O in peralkaline and peraluminous melts. Am. Mineral. 82, 434–437.
Di Vito, M.A., Isaia, R., Orsi, G., Southon, J., de Vita, S., D'Antonio, M., et al., 1999. Volcanic and deformational history of the Campi Flegrei caldera in the past 12 ka. J. Volcanol. Geotherm. Res. 91, 221–246.
Dixon, T.E., Stolper, E., Holloway, J.R., 1995. An experimental study of water and carbon dioxide solubilities in mid-ocean basalt liquids: Part I. Calibration and solubility models. J. Petrol. 36, 1607–1631.
Eggler, D.H., 1972. Water-saturated and water-undersaturated melting relations in a Paricutin andesite and an estimate of water content in natural magma. Contrib. Mineral. Petrol. 34, 261–271.
Gaillard, F., Scaillet, M.B., Pichavant, M., Bény, J.M., 2001. The effect of water and fO_2 on the ferric–ferrous ratio of silicic melts. Chem. Geol. 174, 255–273.
Goranson, R.W., 1931. The solubility of water in granitics magmas. Am. J. Sci. 22, 481–502.
Goranson, R.W., 1936. Silicate–water systems: the solubility of water in albite-melt. Trans.-Am. Geophys. Union 17, 257–259.
Hamilton, D.L., Burnham, C.W., Osborn, E.F., 1964. The solubility of water and effects on fugacity and water content on crystallization in mafic magmas. J. Petrol. 5, 21–39.
Holtz, F., Behrens, H., Dingwell, D.B., Taylor, R.P., 1992. Water solubility in aluminosilicate melts of haplogranite composition at 2 kbar. Chem. Geol. 96, 289–302.
Holtz, F., Behrens, H., Dingwell, D.B., Wilhelm, J., 1995. H_2O solubility in haplogranitic melts: compositional, pressure and temperature dependence. Am. Mineral. 80, 94–108.
Keppler, H., Bagdassarov, N.S., 1993. High-temperature FTIR spectra of H_2O in rhyolite melt to 1300 °C. Am. Mineral. 78, 1324–1327.
Kohn, S.C., Dupree, R., Golam Mortuza, M., 1992. The interaction between water and aluminosilicate magmas. Chem. Geol. 96, 399–409.
Kushiro, I., 1972. Effect of water on the composition of magmas formed at high pressures. Am. J. Sci. 267A, 269–294.
Kushiro, I., 1978. Density and viscosity of hydrous calc-alkalic andesite magma at high pressure. Year B.-Carnegie Inst. Wash. 77, 675–678.
Lange, R.A., Carmichael, I.S.E., 1987. Densities of Na_2O-K_2O-CaO-MgO-FeO-Fe_2O_3-Al_2O_3-TiO_2-SiO_2 liquids: new measurements and derived partial molar properties. Geochim. Cosmochim. Acta 51 (11), 2931–2946.
Lebedev, E.E., Khitarov, N.I., 1964. The dependence of electrical conductivity of granite melt and the beginning of granite melting on high pressure of water. Geokhimiya 3, 195–201 (in Russian).
McMillan, P.F., 1994. Water solubility and speciation models. In: Carroll, M.R., Holloway, J.R. (Eds.), Volatiles in Magmas. Rev. Miner., vol. 30, p. 517.
Moore, G., Vennemann, T., Carmichael, I.S.E., 1995. Solubility of water in magmas to 2 kilobars. Geology 23, 1099–1102.
Moore, G., Vennemann, T., Carmichael, I.S.E., 1998. An empirical model for the solubility of H_2O in magmas to 3 kilobars. Am. Mineral. 83, 36–42.
Newman, S., Stolper, E.M., Epstein, S., 1986. Measurement of water in rhyolitic glasses: calibration of an infrared spectroscopic technique. Am. Mineral. 71, 1527–1541.
Nowak, M., Berhens, H., 1995. The speciation of water in haplogranitic glasses and melts determined by in situ near-infrared spectroscopy. Am. Mineral. 59 (16), 3445–3450.
Nowak, M., Berhens, H., 2001. Water in rhyolitic magmas: getting a grip on a slippery problem. Earth Planet. Sci. Lett. 184, 515–522.
Nowak, M., Berhens, H., Johannes, W., 1996. A new type of high-temperature, high pressure cell for spectroscopic studies of hydrous silicate melts. Am. Mineral. 81, 1507–1512.
Ohlhorst, S., Behrens, H., Holtz, F., 2001. Compositional dependence of molar absorptivities of near-infrared OH- and H_2O bands in rhyolitic to basaltic glasses. Chem. Geol. 174, 5–20.
Orlova, G.P., 1962. The solubility of water in albite melts. Int. Geol. Rev. 6 (1964), 254–258.
Osborn, E.F., 1959. The role of oxygen pressure in the crystallization and differentiation of basaltic magma. Am. J. Sci. 257, 609–647.
Ostroviskiy, I.A., Orlova, G.P., Rudnitskaya, Y.S., 1964. Stoichiometry in the solution of water in alkali-aluminosilicate melts. Dokl. Akad. Nauk SSR 157, 149–151.
Papale, P., 1997. Thermodynamic modeling of the solubility of H_2O and CO_2 in silicate liquids. Contrib. Mineral. Petrol. 126, 237–251.
Pappalardo, L., Piochi, M., D'Antonio, M., Civetta, L., Petrini, R., 2002. Evidence for multi-stage magmatic evolution during the past 60 ka at Campi Flegrei (Italy) deduced from Sr, Nd and Pb isotope data. J. Petrol. 43 (8), 1415–1434.
Richet, P., Lejeune, A.M., Holtz, F., Roux, J., 1996. Water and the viscosity of andesite melts. Chem. Geol. 128, 185–197.
Richet, P., Whittington, A., Holtz, F., Behrens, H., Ohlhorst, S., Wilke, M., 2000. Water and the density of silicate glasses. Contrib. Mineral. Petrol. 138, 337–347.

Rosi, M., Sbrana, A., 1987. Phlegrean fields. CNR, Quad. Ric. Sci. 114, 1–175.

Rossman, G.R., 1988. Optical spectroscopy. In: Hatworne, F.C. (Ed.), Spectroscopic methods in Mineralogy and Geology. Rev. Mineral., vol. 18, pp. 207–243.

Schmidt, B.C., Riemer, T., Kohn, S.C., Behrens, H., Dupree, R., 2000. Different water solubility mechanism in hydrous glasses along the Qz–Ab join: evidence from NMR spectroscopy. Geochim. Cosmochim. Acta 64 (3), 513–526.

Schmidt, B.C., Riemer, T., Kohn, S.C., Holtz, F., Dupree, R., 2001. Structural implications of water dissolution in haplogranitic glasses from NMR spectroscopy: influence of total water content and mixed alkali effect. Geochim. Cosmochim. Acta 65 (17), 2949–2964.

Scholze, H., 1960. Zur Frage der Unterscheidung zwischen H_2O-Molekelen und OH-Gruppen in Gläsern und Mineralen. Naturwissenschaften 47, 226–227.

Shen, A., Keppler, H., 1995. Infrared spectroscopy of hydrous silicate melts to 1000 °C and 10 kbar—direct observation of H_2O speciation in a diamond-anvil cell. Am. Mineral. 80, 1335–1338.

Silver, L.A., Ihinger, P.D., Stolper, E., 1990. The influence of bulk composition on the speciation of water in silicate glasses. Contrib. Mineral. Petrol. 104, 142–162.

Stolper, E., 1982a. The speciation of water in silicate melts. Geochim. Cosmochim. Acta 46, 2609–2620.

Stolper, E., 1982b. Water in silicate glasses: an infrared spectroscopy study. Contrib. Mineral. Petrol. 81, 1–17.

Tamic, N., Behrens, H., Holtz, F., 2001. The solubility of H_2O and CO_2 in rhyolitic melts in equilibrium with a mixed CO_2–H_2O fluid phase. Chem. Geol. 174, 333–347.

Watson, E.B., 1994. Diffusion in volatile-bearing magmas. In: Carroll, M.R., Holloway, J.R. (Eds.), Volatiles in Magmas. Rev. Miner., vol. 30, pp. 371–411.

Whiters, A.C., Zhang, Y., Behrens, H., 1999. Reconciliation of experimental results on H_2O speciation in rhyolitic glass using in-situ and quenching techniques. Earth Planet. Sci. Lett. 173, 343–349.

Yamashita, S., Kitamura, T., Kusakabe, M., 1997. Infrared spectroscopy of hydrous glasses of arc magma composition. Geochem. J. 31, 169–174.

Yoder Jr., H.S., 1969. Calc-alkalic andesites: experimental data bearing on the origin of their assumed characteristics. In: McBirney, A.R. (Ed.), Proceedings of the Andesite Conference. Or. Dep. Geol. Miner. Ind. Bull., vol. 65, pp. 77–89.

Yoder Jr., H.S., 1973. Contemporaneous basaltic and rhyolitic magmas. Am. Mineral. 58, 153–171.

Zeng, Q., Nekvasil, H., Grey, C.P., 2000. In support of a depolymerization model for water in sodium aluminosilicate glasses: information from NMR spectroscopy. Geochim. Cosmochim. Acta 64 (5), 883–896.

Zhang, Y., 1999. H_2O in rhyolitic glasses and melts: measurement, speciation, solubility and diffusion. Rev. Geophys. 37, 493–516.

Zhang, Y., Stolper, E.M., Ihinger, P.D., 1995. Kinetics of the reaction $H_2O+O=2OH$ in rhyolitic and albitic glasses: preliminary study. Am. Mineral. 80, 593–612.